University of Reading

Vertical structure of stratospheric water vapour trends derived from merged satellite data

Article

Accepted Version

Hegglin, M.I. ORCID: https://orcid.org/0000-0003-2820-9044, Plummer, D.A., Shepherd, T.G. ORCID: https://orcid.org/0000-0002-6631-9968, Scinocca, J.F., Anderson, J., Froidevaux, L., Funke, B., Hurst, D., Rozanov, A., Urban, J., von Clarmann, T., Walker, K.A., Wang, H.J., Tegtmeier, S. and Weigel, K. (2014) Vertical structure of stratospheric water vapour trends derived from merged satellite data. Nature Geoscience, 7 (10). pp. 768-776. ISSN 1752-0894 doi: https://doi.org/10.1038/ngeo2236 Available at https://centaur.reading.ac.uk/37807/

It is advisable to refer to the publisher's version if you intend to cite from the work. See Guidance on citing.

To link to this article DOI: http://dx.doi.org/10.1038/ngeo2236

Publisher: Nature Publishing Group

All outputs in CentAUR are protected by Intellectual Property Rights law, including copyright law. Copyright and IPR is retained by the creators or other copyright holders. Terms and conditions for use of this material are defined in the End User Agreement.

University of Reading

www.reading.ac.uk/centaur

CentAUR

Central Archive at the University of Reading

Reading's research outputs online

Vertical structure of stratospheric water vapour trends derived from merged satellite data

M. I. Hegglin, D. A. Plummer, T. G. Shepherd, J. F. Scinocca, J. Anderson, L. Froidevaux, B. Funke, D. Hurst, A. Rozanov, J. Urban, T. von Clarmann, K. A. Walker, R. Wang, S. Tegtmeier, and K. Weigel

Stratospheric water vapour is a powerful greenhouse gas and knowledge of its long-term behaviour is crucial to understand climate change. The longest available record from balloon observations over Boulder shows increases in stratospheric water vapour which cannot be fully explained by observed changes in its main drivers, tropical tropopause temperatures and methane. Although satellite observations could help resolve the conundrum, constructing a reliable long-term data record is challenging. Here we introduce a new data merging approach using a chemistry-climate model nudged to observed meteorology as a transfer function between satellite datasets, overcoming issues arising from instrument drifts and short overlap periods. In the lower stratosphere, the resulting water-vapour record is extended back to 1988 and largely follows tropical tropopause temperatures. Lower and mid-stratospheric long-term trends are negative rather than positive, with Boulder trends shown not to be globally representative. In the upper stratosphere, the record is extended back to 1986 and shows positive long-term trends. The altitudinal differences in the trends are explained by methane oxidation together with a strengthened lower-stratospheric and weakened upper-stratospheric circulation inferred by this analysis. Our results call into question previous estimates of surface radiative forcing based on presumed long-term global lower-stratospheric water-vapour increases.

Recent experiences with climate data records suggest that there is nothing like 'the ultimate climate data record' and that different approaches to dataset construction are needed to estimate the uncertainty introduced by the construction process itself. For example, upper-tropospheric warming was underestimated by Microwave-Sounding Unit Channel 2 temperature due to the influence of a priori information and the coarse vertical resolution of the retrieval[1]. More recently, it has been argued[2] that the apparent hiatus in global-mean warming is an artefact of sampling biases in the global network of surface data used to estimate global mean temperature changes. Both examples illustrate the limitations of observational datasets with gaps filled by statistical relationships.

An important climate data record is stratospheric water vapour, which exerts a strong radiative forcing affecting temperatures both locally[3] and at Earth's surface[4,5]. Through thermal-wind balance, stratospheric temperature changes are believed to affect the stratospheric circulation and, through dynamical coupling, surface climate[6,7]. Long-term changes in extratropical lower-stratospheric water vapour derived from balloon measurements at Boulder (the longest available record[8]) from 1980-2010 show an average increase of 1.0±0.2 ppmv in the 16-26

km altitude range[9,10]. About 25-30% of this increase has been attributed to methane oxidation[10,11]. The rest remains unexplained, since tropical tropopause temperatures (another key driver of long-term changes[12]) exhibit trends that are not significantly different from zero over this period[13,14]. Comparison of the Boulder record with HALOE satellite measurements, which exhibit essentially a zero long-term trend from 1992-2005, shows discrepancies in the early 1990s[15]. However, there is a possibility that the HALOE record suffers from aerosol contamination or long-term drifts[16].

The observed records of stratospheric water vapour thus present a conundrum. As a result, confidence in global long-term trends is low[17,18]. The difficulty in quantifying stratospheric water-vapour trends arises from limitations of observational systems in the face of strong interannual and decadal variability[15,19,20]. There is general agreement that upper-tropospheric and lower-stratospheric humidity measurements from the global radiosonde network cannot be trusted[21]. Balloon-borne frostpoint hygrometers are characterized by high accuracy and precision[22], but their measurement records are temporally and spatially sparse. Satellite instruments offer global coverage but have finite lifetimes, so different datasets need to be merged into long-term records, often without much overlap. Even with overlapping datasets, the merging may introduce temporal inhomogeneities since aging instruments can show degradation in performance.

New approach to merge stratospheric water vapour datasets

We introduce a new approach to investigate long-term trends in stratospheric water vapour, using timeseries from a state-of-the art chemistry-climate model nudged to observed meteorology (but not water vapour) from the ERA-Interim reanalysis over 1980-2010 (CMAM30) as a transfer function between satellite datasets. This approach exploits the extensive effort made in developing stable reanalysis products, with ERA-Interim now exhibiting a much better representation of the stratospheric circulation than earlier products[21]. The resulting CMAM30 stratospheric water vapour is expected to provide a reasonable long-term reference since it includes the main known transport, mixing, microphysical (dehydration at the tropical tropopause and in polar regions), and chemical processes (in particular methane oxidation) affecting its distribution and long-term changes. Although the model is not assumed to be correct in absolute terms, its use as a transfer function allows relative biases between satellite instruments to be determined using all available measurements, not just those restricted to overlap periods, thereby improving the characterization of inter-instrument biases and allowing the identification of potential instrumental drifts or sampling issues. Consistency between model and measurements suggests that the processes controlling stratospheric water vapour are sufficiently well understood to explain the long-term changes, and that CMAM30 can be trusted as a transfer function, while inconsistencies point out weaknesses either in the model or observations. The temporal homogeneity of the water-vapour record can also be tested by examining the consistency of its long-term changes with those of other variables. Using this

knowledge, the observational datasets can more confidently be used to create long-term data records.

As an application of the approach, we merge zonal monthly-mean water-vapour timeseries from seven limb-viewing satellite instruments compiled and quality assessed by the SPARC Data Initiative[23] into a long-term record. *Figure 1a* shows the individual satellite timeseries at 100 hPa for 20S-20N and the large discrepancies between them. Relative biases to CMAM30 are calculated for each instrument (*Figure 1b*), avoiding periods where the instruments have known problems (see Supplementary Material). The post-2006 period is excluded from the relative-bias calculation because of a known inhomogeneity in ERA-Interim lower-stratospheric temperatures in late 2006 due to the introduction of GPS radio-occultation data[24] (see *Supplementary Material, Table 1*). Overall, the relative biases are seen to be well defined (as shown in scatter plots in *Supplementary Figure S1*), yielding confidence in the ability of CMAM30 to represent water-vapour variability, and thus in its use as a transfer function between datasets. Using CMAM30 as a transfer function, each instrument record is then adjusted relative to Aura-MLS (*Figure 1d*).

There is a potential pitfall in this approach in that long-term changes in the merged dataset could be influenced by the long-term trend in the model. This possibility is assessed by examining whether there are apparent drifts in the model-measurement differences over time, or jumps between the older (SAGE II and HALOE) and newer instruments following the bias correction (*Figure 1c*). For the most part, the differences between these bias-corrected timeseries and CMAM30 are stable in time, suggesting that there is no artificial long-term trend introduced by this procedure. That the differences are stable over the SAGE II record furthermore indicates very good long-term stability of these observations, despite earlier concerns about a drift in the instrument's retrieval channel[25]. This suggests that SAGE II can be used to extend the satellite water-vapour record back to the mid-1980s. Distinct low biases are found for HALOE during 1993-1995, which are likely due to aerosol interference in the retrieval after the Mt. Pinatubo eruption, and during 2003-2005, confirming previous comparisons[16,20]. Similarly, the last year of SAGE II data (2005) seems to exhibit a low bias. The earlier MIPAS data (2002-2004) indicate a slight low bias with respect to the later MIPAS data (2005-2010), as also found in Ref 23. The remaining fluctuations reveal mostly differences in how the instruments resolve the amplitude of the seasonal cycle, likely attributable to differing vertical resolutions of the observations[23]. The bias-corrected timeseries show a coherent evolution of tropical lower-stratospheric water vapour (*Figure 1d*), with no evidence of a jump between the older and newer instruments — further evidence that the procedure has not introduced any artificial long-term trend. A merged satellite stratospheric water-vapour record is finally produced by calculating the multi-instrument mean of all available bias-corrected datasets (however excluding HALOE during 2003-2005 and SAGE II during 2005 due to their identified low biases).

Consistency with tropical tropopause temperatures

In the lower stratosphere, water vapour is known to broadly follow variations in tropical tropopause temperatures[15,16,17,19,20,27,28]. The merged record is therefore compared to temperature fluctuations, using deseasonalized anomalies normalized by the standard deviation of the respective variable's interannual variability in order to make them comparable and check their consistency (*Figure 2a*). We here use the CMAM30 100 hPa temperature averaged over 15S-15N, which has been shown to vary coherently with cold-point tropopause temperatures[19,28], and emphasize again that the variability and trends of the individual datasets are unaffected by the bias correction and thus not influenced by the model. The 80 hPa water-vapour anomalies derived from the merged satellite record (at this level representative of purely stratospheric air) strongly follow the temperature fluctuations, with a correlation coefficient (R) (or variance explained) of 0.77 (59%) over the full time period, which increases to 0.89 (78%) when considering only 2001 onwards (likely explained by the better spatio-temporal coverage provided by the newer instruments, resulting in more representative zonal monthly means). The consistency between the temperature and water-vapour datasets is further highlighted by plotting the normalized differences (or residuals) of their anomalies (*Figures 2b and c*), for which the inter-annual variability is much reduced.

Consistency between the merged water-vapour record and tropical tropopause temperatures is also found in the extratropical lower stratosphere at 100 hPa (with a lag of two months to account for transport time scales between the tropics and extratropics[28])(*Figures 2d* and *e*), with a correlation coefficient (variance explained) of 0.66 (43%). The normalized differences between water vapour and temperature are somewhat stronger than in the tropics, due to enhanced dynamical variability and its effect on tracer transport and mixing with older stratospheric air at these latitudes. Dehydration in the polar vortex may also contribute[29]. The good agreement between measurements and model (*Figure 2e*) shows that these additional processes are adequately represented in the model. Nevertheless, the low-frequency variability of extratropical lower-stratospheric water vapour seems mainly to arise from the variability of tropical tropopause temperatures.

There are four time periods that show deviations from this strong correlation: 1992-1996 for the observations (but not for the model), which is presumed to be a result of Mt Pinatubo aerosol affecting the water-vapour retrieval[16]; and 1999-2000, 2003, and 2008-2009. The causes of the latter are not known but since they occurred in both observations and model they are presumed to be real.

The new merged water-vapour record appears to be an improvement over a previous merge of the HALOE and Aura-MLS data sets based only on the relative bias during their 16 months of overlap[16,17,30], since the latter record shows a temporal inhomogeneity in deviations from the temperature record (*Figures 2c,e*). As discussed above, HALOE exhibits a low bias in the lower stratosphere during its final years of operation that may adversely affect a long-term data record

constructed by merging HALOE with another dataset such as Aura-MLS during this period. Our approach, in contrast, shows that taking the long-term behaviour of the datasets into account substantially improves the consistency between the water-vapour and temperature records. After the strong dip around 2001, the previous merge of HALOE and Aura-MLS only partially recovers by 2010 (Refs 30,31), while the merged record using CMAM30 recovers fully to pre-2001 values by 2007. Calculations of surface radiative forcing from changes in lower-stratospheric water vapour based on the simple merge of HALOE and Aura-MLS[30] may thus overestimate the cooling effect on global mean surface temperatures after 2001.

Comparison with in-situ observations over Boulder

We now turn to the question of the apparent inconsistency between the long-term Boulder FPH balloon and satellite datasets[15,17]. We investigate whether the Boulder trends are representative of the Northern Hemisphere mid-latitude stratosphere by sub-sampling the model at the location (40N/105W) and time of the Boulder measurements. *Figure 3a* shows Boulder 100 hPa water-vapour anomalies extending back to 1980 together with the full and subsampled anomalies derived from the model. The agreement between the merged satellite and full model datasets back to 1988 provides confidence that the model exhibits a correct representation of inter-annual variability and long-term changes in stratospheric water vapour. The sub-sampled model fields generally correlate better with the Boulder in-situ measurements than do the full model fields in terms of year-to-year fluctuations, explaining the differences between the Boulder and (zonal-mean) satellite observations during some years (e.g., 1988-1992, 1997-1998, and 2003-2005). Nevertheless, the 100 hPa change over 1980-2010 derived from the sub-sampled model fields (-0.27±0.18 ppmv) disagrees with that from Boulder (0.6±0.15 ppmv). The difference is smaller, but still statistically significant (-0.15±0.22 ppmv compared with 0.39±0.18 ppmv), over 1988-2010 where the zonal-mean model trend is consistent with that of the merged satellite record. The differences from the near-global water-vapour fields (*Figure 3b*) illustrate in more detail the close agreement between the sub-sampled and Boulder water-vapour records, except for the three time periods highlighted in red which together lead to the differences in their long-term trends. Inspection of the model's longitude-latitude distribution of water-vapour changes indicates that these are not longitudinally uniform (*Figure 3c*). Positive trends are found south-west of Boulder, with the limited spatial resolution of the model likely missing the full extent of the geographical structure and temporal variability of this feature. Our results suggest that the water-vapour trends over Boulder should not be considered representative of the global stratosphere.

Long-term stratospheric water-vapour changes

Figure 4a shows the bias-corrected individual water-vapour datasets at 10 hPa in the extratropics together with the model-instrument biases (*Figure 4b*). Our method reveals minor discrepancies between two available SAGE II data versions (see Supplementary Material). HALOE shows no apparent low bias as was identified in the lower stratosphere for its last years of operation, showing that satellite instrument biases and drifts can be latitude- and altitude-dependent. While the model exhibits a strong low bias at this altitude, its long-term evolution and inter-annual variability show very good agreement with the observations back to 1986 (*Figure 4c*). This level of agreement provides confidence in the ERA-Interim reanalysis driving the model while at the same time highlighting once again the high quality of the SAGE II data, suggesting that the satellite water-vapour record can be extended back to the mid-1980s. (See *Supplementary Figure S3* for more examples.)

Figure 5a shows the long-term changes between the late 1980s and 2010 derived from the merged satellite record throughout the stratosphere, and *Table 1* quantifies the long-term changes shown in the different figures. The trends are significantly positive in the upper stratosphere, while the lower and mid-stratosphere show significant negative trends (in contrast to the Boulder observations). This vertical structure in the long-term trends is found at all latitudes. In the tropical tropopause region around 80 hPa, a negative long-term trend is identified with 70% significance. On the other hand, positive changes of more than 10% are found in the tropical upper troposphere. While these latter two findingsneed to be treated with caution due to sampling limitations, they are in broad agreement with past trends derived from chemistry-climate model simulations[12,32].

The observed water-vapour changes are now attributed to different drivers using the well-established "total water" diagnostic[33,34,16] (see *Methods* and *Supplementary Material*). The contribution from methane entry-value changes is shown in *Figure 5b*, and is derived from tropospheric observations of methane changes together with a fractional-release factor (α) (*Supplementary Figure S3*) inferred from ACE-FTS stratospheric methane measurements. The contribution varies smoothly from zero in the tropical lower stratosphere to approximately 3% of water vapour in the upper stratosphere, the latter representing a significant fraction of the observed water-vapour increase (*Figure 5a*). The contribution from water-vapour entry-value changes is obtained from the merged 80 hPa record shown in *Figure 2a*, and is a constant -0.14±0.2 ppmv (hence not plotted). Assuming conservation of total water, the difference between the sum of those two contributions and the observed change can be attributed to changes in α, representing a change in stratospheric circulation, whose inferred contribution to the observed water-vapour change is shown in *Figure 5c*. This contribution is negative in the lower stratosphere and positive in the upper stratosphere. The breakdown of the different contributions is shown in *Figure 5d* together with their uncertainties for three locations with particularly large long-term water-vapour changes. The uncertainty in the inferred contribution from circulation changes is dominated by the large uncertainty in the water-vapour entry-value changes because of the large inter-annual variability of the latter (*Figure*

2a). However, the difference between the inferred contributions in the upper and lower stratosphere is robust because the same water-vapour entry-value change is used for both, and it is not possible to explain the observed water-vapour changes, within uncertainties, without the inferred circulation changes. In the northern high-latitude upper stratosphere (5 hPa, 62.5N) the long-term increase of 0.28 ppmv is due in equal measure to methane increase and α increase, with an offset from the decreasing water-vapour entry value. In the midlatitude lower stratosphere of both hemispheres (30 hPa, 42.5N and 50 hPa, 43.5S), long term decreases of -0.28 and -0.34 ppmv respectively are mainly explained by decreasing α, with an additional contribution from the decreasing water-vapour entry value and a small offset from the methane increase. Thus, the different drivers affect the water-vapour changes differently in different regions.

Larger α corresponds to older age-of-air. To facilitate comparison with observed estimates of long-term circulation changes, we determine an approximate relationship between the two quantities (*Supplementary Figure S5*), and use it to translate the inferred α changes into age-of-air changes (*Figure 5e*). This shows a strong decrease in age-of-air in the lower stratosphere, and a weak increase in the upper stratosphere, which is broadly consistent with the evidence for both tendencies in long-term observations of stratospheric trace gases[35,36,37]. An increased strength of the lower-stratospheric circulation is also consistent with chemistry-climate model simulations[38], likely exacerbated in past decades by the effect of the ozone hole, which will reverse sign in the future[39].

Improved knowledge of stratospheric water-vapour changes

We have introduced a novel method to generate a long-term record of stratospheric water vapour, using a chemistry-climate model nudged to observed meteorology to provide a transfer function between the available satellite datasets. This approach provides an improved assessment of the relative biases between instruments, potential instrumental drifts, as well as possible sampling biases, compared to what is possible from the observations alone, especially for instruments with no or small overlap in time.

The new merged satellite water-vapour record extends back to the late 1980s and shows long-term decreases in the lower and mid-stratosphere, in contrast to the Boulder record which is shown not to be globally representative. Upper-stratospheric water vapour instead shows a long-term increase. The contributions of the two recognized drivers of water-vapour changes — the stratospheric entry values of water vapour and of methane — are quantified and shown not to be sufficient to explain the observed water-vapour trends, particularly the difference in the trends between the upper and lower stratosphere. The discrepancy is attributed to changes in the fractional-release factor between methane and water vapour, which imply a strengthened lower-stratospheric circulation (reduced age-of-air) and a weakened upper-stratospheric circulation (increased age-of-air), consistent

with other evidence. It hence appears necessary to consider long-term changes in the stratospheric circulation when interpreting changes in stratospheric water vapour, together with changes in methane and water-vapour entry values.

Our results show the value of using models and measurements together to understand the interannual and long-term behaviour of stratospheric water vapour, with the approach being applicable in principle to other trace gases. They also highlight the need for independent and redundant global measurement systems characterized by high long-term accuracy (and precision) to be able to quantify long-term changes in stratospheric water vapour with more confidence.

Acknowledgements

We acknowledge the Canadian Space Agency for having funded the CMAM30 project, with additional institutional support from the Canadian Centre for Climate Modelling and Analysis who provided the model code and supercomputing time. We thank all national and international space agencies for making available their limb satellite observations for use in the SPARC Data Initiative.

Author contributions

M.I.H. designed the methodology, performed the data analysis, and wrote the paper. D.A.P. helped with the statistical analysis and together with J.F.S. devised and implemented the nudged model simulations. T.G.S contributed to the interpretation and writing of the text. D. H. provided processed balloon observations. J. A., L. F., B. F., A. R., J. U., T. v. C., H. J. W., K. A. W., S. T. and K. W. processed and provided the satellite datasets.

Additional information

Supplementary material is provided. Correspondence and request for materials should be addressed to M.I.H.

Competing financial interests

The authors declare no competing financial interests.

FIGURES

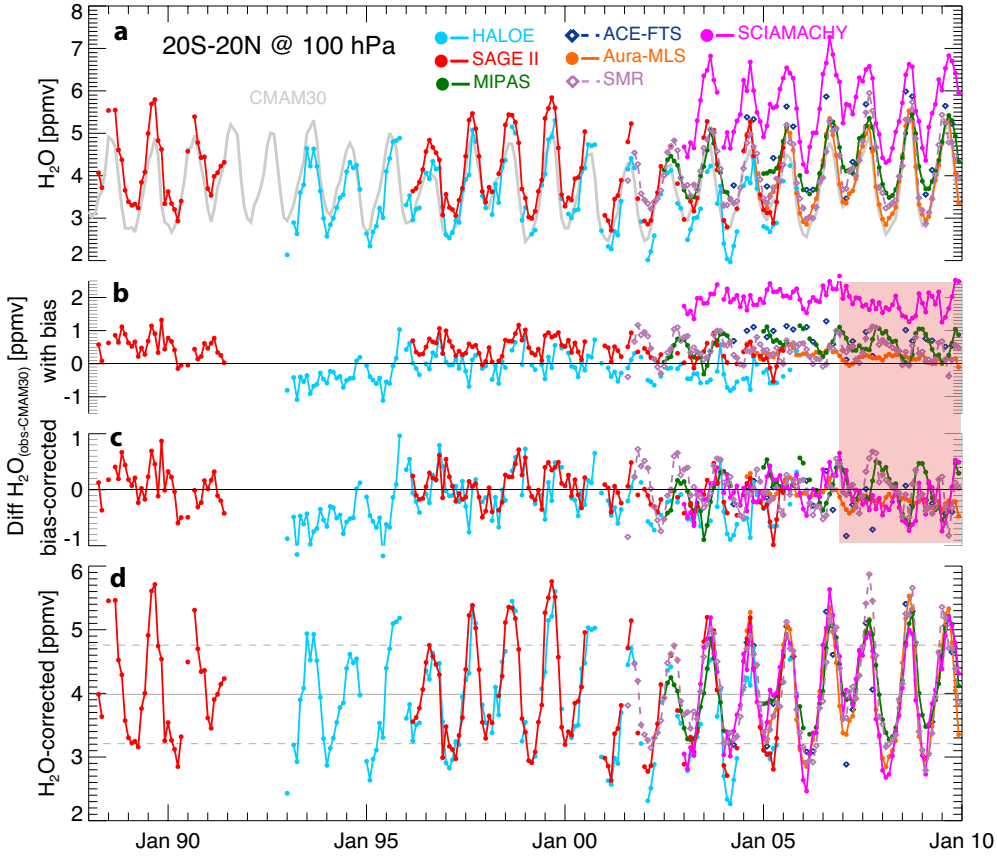

Figure 1: Approach to merging a climate data record. Timeseries of monthly zonal mean water vapour at 100 hPa averaged over 20S-20N for 1988-2010: **(a)** Absolute mixing ratios from different instruments (colours) and CMAM30 (grey), **(b)** differences and **(c)** bias-corrected differences between observations and CMAM30, and **(d)** bias-corrected absolute mixing ratios from observations. Grey solid and dashed horizontal lines in (d) indicate mean and 1-sigma standard deviation of the observational record averaged over the whole time period. The red box encompasses months excluded from the relative-bias determination due to identified problems in ERA-Interim (see text). See Supplementary Material for SCIAMACHY bias explanation.

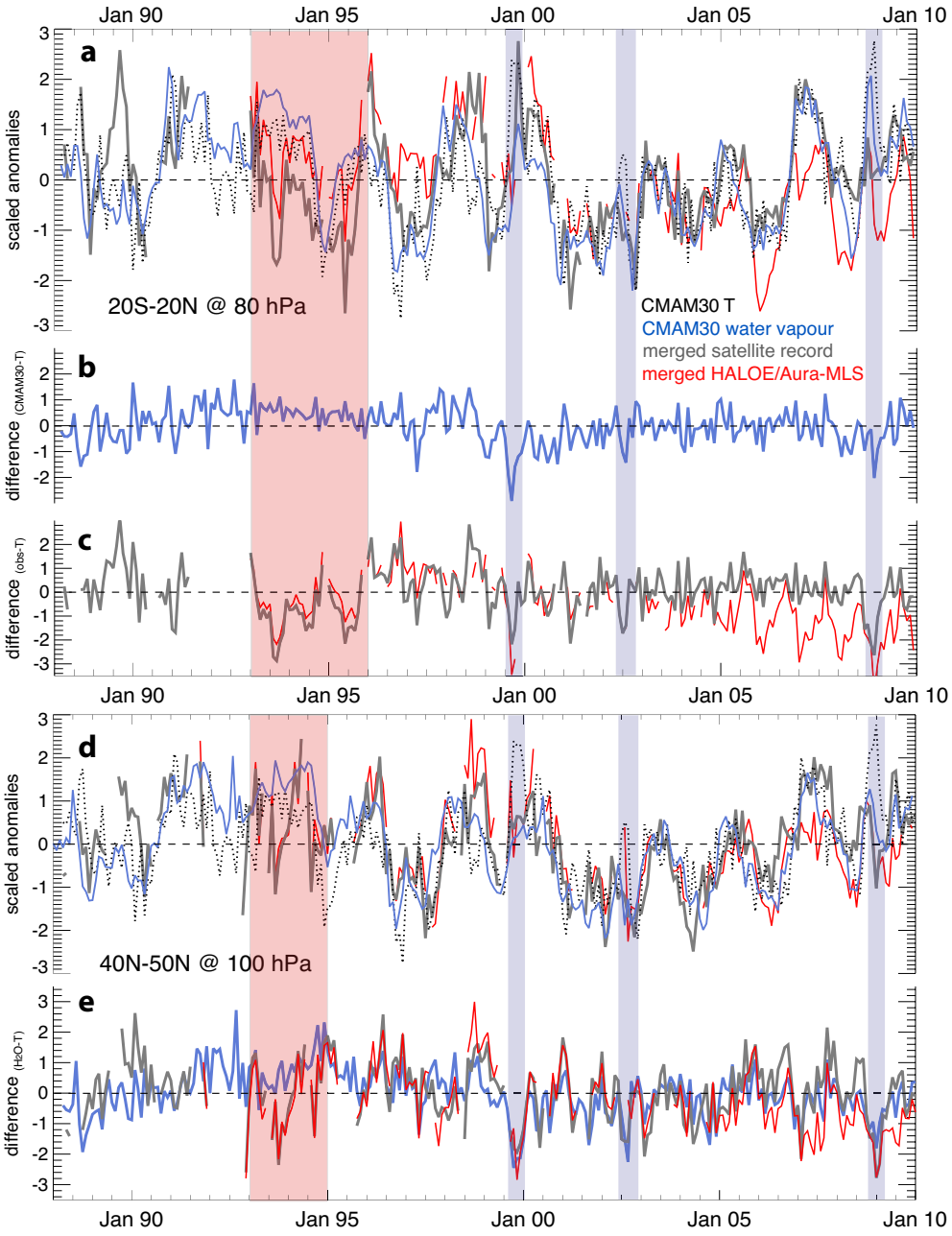

Figure 2: Consistency between tropical tropopause temperature and lower-stratospheric water vapour. Scaled anomalies (unitless) of tropical temperature at 100 hPa averaged over 15S-15N and of water vapour at **(a)** 80 hPa averaged over 20S-20N and **(d)** 100 hPa averaged over 40N-50N. Tropical temperature is lagged by 2 (3) months in the tropics (extratropics). **(b, c,** and **d)** Differences between scaled temperature and water-vapour anomalies (unitless). Red bar highlights a time period where the scaled anomalies in the model and the observations show a substantial disagreement, blue bars where the temperature-water vapour relationship is strongly perturbed in both model and observations.

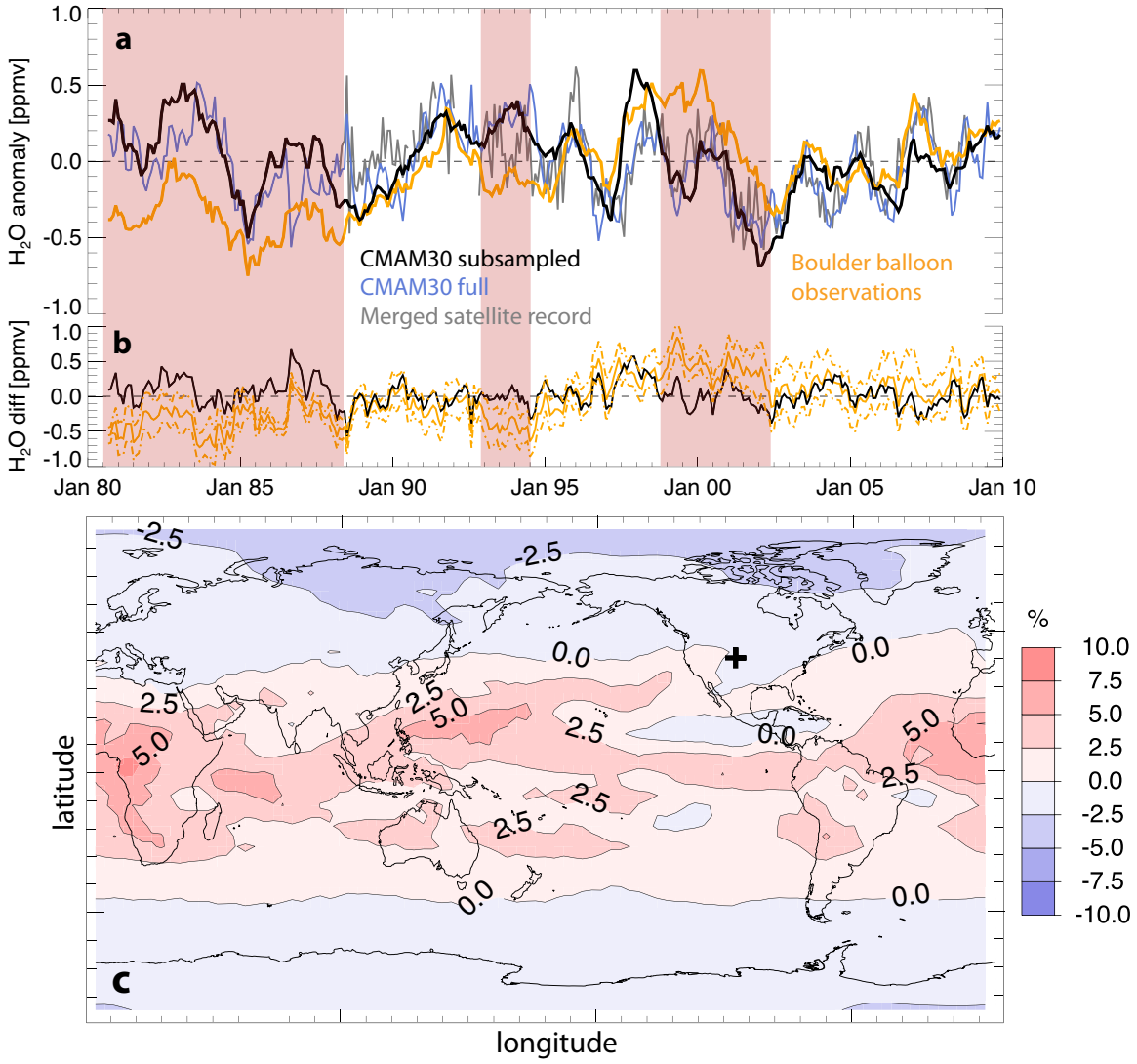

Figure 3: Comparison of stratospheric water vapour from Boulder balloon and merged satellite datasets. (a) Deseasonalized water-vapour anomalies at 100 hPa derived from Boulder balloon observations (orange), the zonal mean (40N-50N) model (blue) and merged satellite data (grey), and the model subsampled at Boulder (black). **(b)** Differences between full model anomalies and balloon (orange) or sub-sampled model anomalies (black). Red shadings highlight periods where sub-sampled model data systematically lie outside the 1-sigma uncertainty of the balloon observations (dashed orange lines). **(c)** Longitude-latitude percentage changes of water vapour at 100 hPa for 1980-2010 from the model. The cross indicates the location of Boulder (40N/105W).

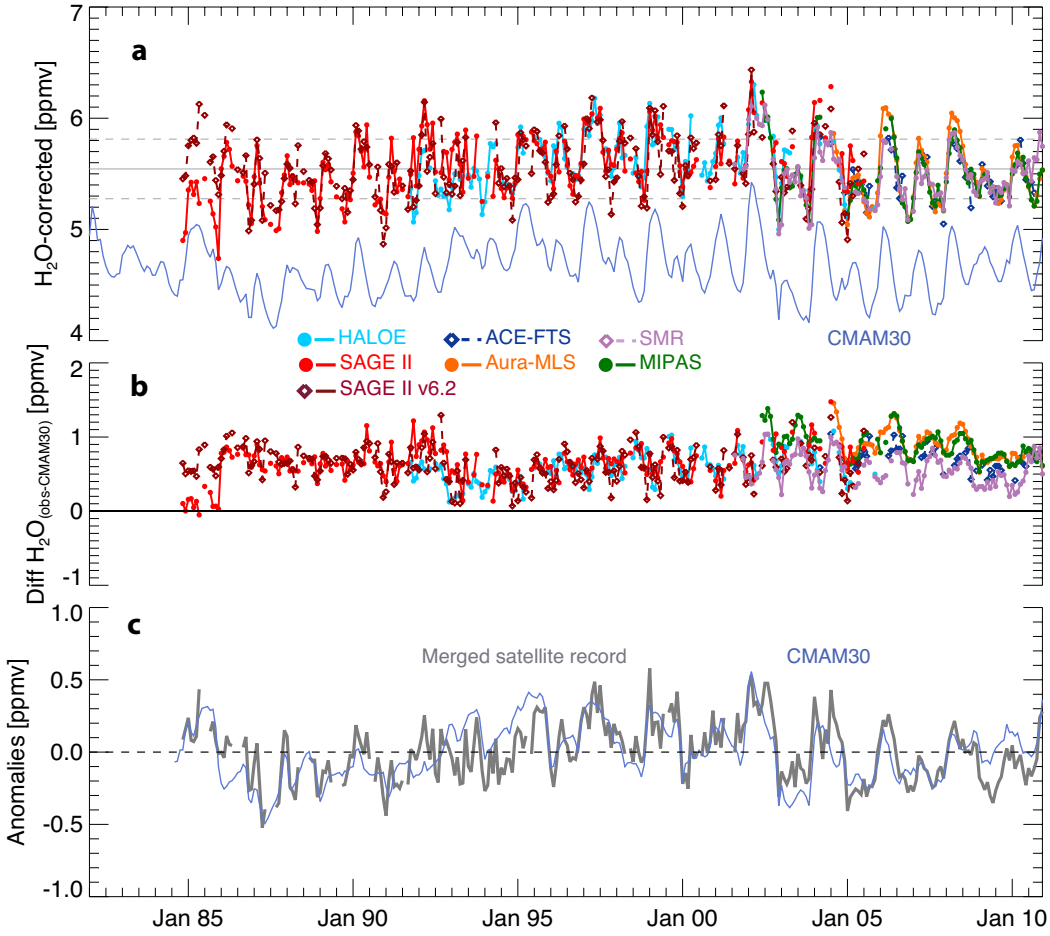

Figure 4: **Extension of the water-vapour timeseries back to the mid 1980s. (a)** Timeseries of zonal mean water vapour at 10 hPa and 40N for model (grey) and the different instruments (bias-corrected and colour-coded). **(b)** Relative biases between each instrument's original monthly zonal mean timeseries and CMAM30. **(c)** Deseasonalized anomalies of the merged satellite water-vapour record (grey) and the model.

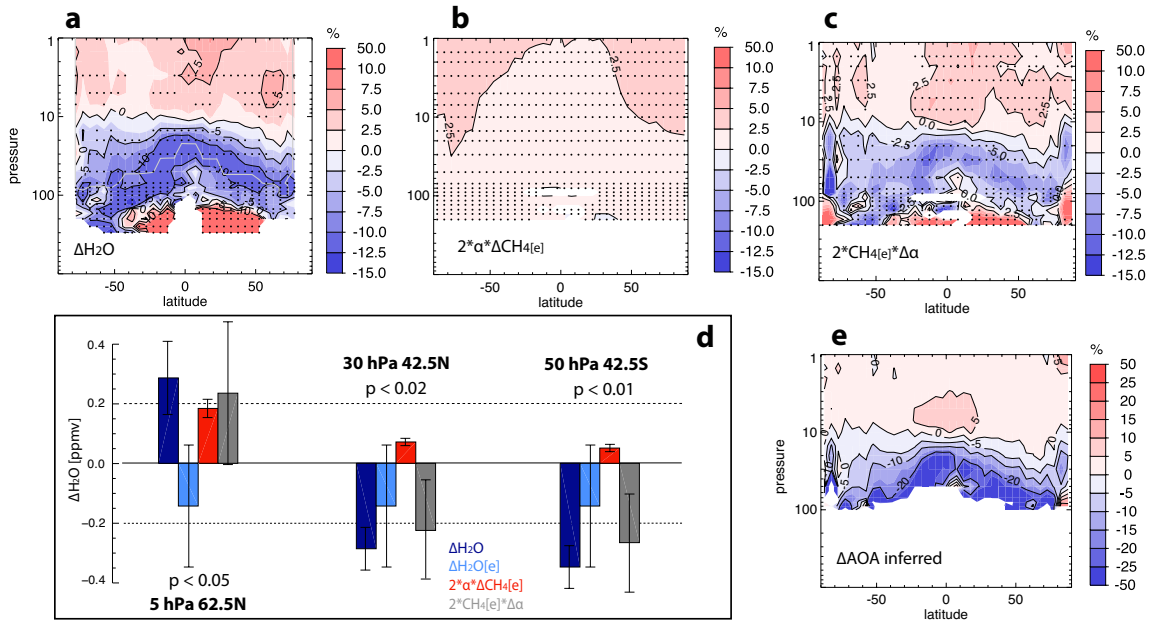

Figure 5: Long-term changes in stratospheric water vapour and its drivers. (a) Percentage changes up to 2010 derived from the merged satellite record since 1986/1988 above/below grey line. Dots indicate 95%-significance level. Contribution to (a) from **(b)** tropospheric methane increases and **(c)** inferred changes in the stratospheric circulation. **(d)** Absolute water-vapour changes at three locations and contributions from their drivers including uncertainties (as discussed in detail in *Supplementary Material*). P-values are given for the difference between observed changes and the sum of the two entry-value contributions. **(e)** Fractional-release factor changes translated into age-of-air (AOA) changes (significance not estimated).

Table 1: (a) Water vapour and (b) temperature changes derived for different time periods, latitude bands, and altitudes from observations and from CMAM30. Changes are calculated for the timeseries shown in *Figures 2, S1, 3*, and *5* and given as total change in ppmv over the entire period. Most trends are not statistically significant due to large variability in stratospheric water vapour when compared to data record length. Decadal fluctuations strongly affect derived trend values depending on the time period chosen[10,31]. Trend and significance calculation is explained in the Methods section. *CMAM30ss* denotes sub-sampled model fields.

H_2O	Period	Lat Band	Height [hPa]	Change [ppmv]	2-sigma Uncertainty [ppmv]	t-value	Effective Sample #	Significance Level
Figures 2 and S1								
Satellite	1988-2010	20S-20N	80	-0.14	0.20	0.67	26	70%
Satellite	1988-2010	20S-20N	100	0.01	0.14	0.06	53	Not sig

Figure 3								
Satellite	1988-2010	37.5-42.5N	100	-0.05	0.17	0.27	32	Not sig
Boulder	1988-2010	37.5-42.5N	100	0.39	0.18	2.17	129	95%
CMAM30ss	1988-2010	37.5-42.5N	100	-0.15	0.22	0.66	84	Not sig
CMAM30	1988-2010	37.5-42.5N	100	-0.07	0.22	0.32	16	Not sig
Boulder	1980-2010	37.5-42.5N	100	0.60	0.15	3.9	160	95%
CMAM30ss	1980-2010	37.5-42.5N	100	-0.27	0.18	1.49	110	90%
CMAM30	1980-2010	37.5-42.5N	100	-0.12	0.19	0.64	22	Not sig
Figure 5e								
Satellite	1986-2010	62.5N	5	0.28	0.12	2.4	26	95%
Satellite	1986-2010	42.5N	30	-0.28	0.07	4.1	65	95%
Satellite	1986-2010	42.5S	50	-0.34	0.07	5.2	72	95%
Temp	**Period**	**Lat Band**	**Height [hPa]**	**Change [K]**	**2-sigma Uncertainty [K]**	**t-value**	**Effective Sample #**	**Significance Level**
Figure 2								
Model	1988-2010	15S-15N	100	-0.04	0.32	0.13	249	Not sig

436
437
438
439

Methods

Nudged Chemistry-Climate Model simulations . The CMAM30 dataset is produced using the Canadian Middle Atmosphere Model[40] driven by the latest European Centre for Medium-Range Weather Forecasts (ECMWF) ERA-Interim reanalysis[21] over the past 30 years (1980-2010). For details on the nudging see *Supplementary Material*. The model was run on 71 vertical levels from the surface to around 95 km, with a vertical resolution of approximately 1 km around the tropopause, and a horizontal resolution of T47, or approximately 4 degrees. The stratospheric source gas of water vapour, methane, is prescribed as a time-varying, global average surface concentration based on observations and is subject to model transport and chemistry. Water vapour is likewise a fully prognostic field in the model, chemically produced by methane oxidation and removed through parameterized large-scale and deep convective precipitation processes. Water vapour in excess of the local saturation mixing ratio is removed, following the rationale that the stratospheric water-vapour entry value is largely determined by the Lagrangian cold point as air passes through the tropical tropopause[19], but neglecting super-saturation[41]. The free-running CMAM has been evaluated for its performance in the upper troposphere and lower stratosphere both in the tropics[12] and extratropics[42] and found to be one of the best-performing models. CMAM30 data can be downloaded from http://www.cccma.ec.gc.ca/data/cmam/output/CMAM/CMAM30-SD/index.shtml

SPARC Data Initiative timeseries. The SPARC Data Initiative water-vapour timeseries have been compiled using profile data that were carefully screened before binning, and a hybrid log-linear interpolation in the vertical has been performed. The timeseries feature zonal monthly mean cross sections with a horizontal resolution of 5° on 28 pressure levels between 300 and 0.1 hPa (around 64 km altitude). We here use the timeseries from seven instruments, which provide near-global coverage (SAGE II, HALOE, Odin/SMR, SCIAMACHY, ACE-FTS, Aura-MLS, and MIPAS) and have been quality-assessed within the SPARC Data Initiative[23]. Sampling issues are discussed in Ref 43. The climatologies were based on the following data versions (specific references are provided in Ref 23): HALOE v19, SMR v2.0 (in the lower stratosphere) and SMR v2.1 (in the middle and upper stratosphere), SCIAMACHY v3.0, ACE-FTS v2.2, Aura-MLS v3.3, and MIPAS v3o_H2O_13 (for 2002-2004 data) and v5r_H2O_220 (for 2005-2010 data, where the operation mode was switched from high-spectral to low-spectral resolution). SAGE II v6.2 submitted to the SPARC Data Initiative is only shown in *Figure 4*, but otherwise is superseded by climatologies based on the improved SAGE II v7.0 data[43]. For methane, ACE-FTS data[45] were used. The SPARC Data Initiative climatologies can be downloaded from http://www.sparc-climate.org/data-center/data-access/sparc-data-initiative/

Boulder balloon observations. Water vapour vertical profile measurements over Boulder by balloon-borne NOAA frost point hygrometers (FPHs) started in April 1980 and continue today. Most soundings were conducted monthly, however the

record contains several multi-month data gaps, especially above 22 km. A comparison of FPH and Aura-MLS measurements over Boulder and Lauder, New Zealand, shows no significant temporal drifts between the two instruments from 100 to 26 hPa during 2004-2012 (Ref. 46). See also discussion of measurement uncertainty in the *Supplementary Material*.

Anomalies. Anomalies are calculated with respect to the full time period depicted in the different figures, by subtracting the seasonal cycle derived from each individual instrument or the model from the overall time series.

Trends and significance tests. Unless indicated otherwise, uncertainty estimates are given as two sigma throughout the manuscript. We use a least-square linear regression in order to derive the trends from deseasonalized water-vapour anomaly timeseries at the different altitudes and latitudes. The significance of the trend is derived taking into account the effect of potential autocorrelation within the timeseries on the number of independent data points (reducing the effective sample size). This effective sample size is then used to recalculate the uncertainty of the derived trends and determine the tabulated one-sided student's t-test value, used to define the significance level of the trends. A more detailed discussion of the method can be found in Ref 47.

Total-water diagnostic. Apart from polar dehydration and other non-conservative processes, stratospheric "total water" $H_2O + 2{\cdot}CH_4$ is approximately conserved[33,34,16] hence water vapour and methane at a given location can be written as

$$H_2O = H_2O_{[e]} + 2\alpha CH_{4[e]}, \qquad CH_4 = (1-\alpha)\, CH_{4[e]} \tag{1a,b}$$

where the subscript '[e]' refers to the entry value at the tropical tropopause (lagged by the mean age-of-air), and α represents a fractional-release factor which depends on the circulation. Under this assumption, sufficiently small water-vapour changes can be attributed to changes in water-vapour entry value, methane entry value, and circulation according to

$$\Delta H_2O = \Delta H_2O_{[e]} + 2\alpha\Delta CH_{4[e]} + 2CH_{4[e]}\Delta\alpha\,. \tag{2}$$

The calculation of α and $\Delta CH_{4[e]}$ and their uncertainties is described in the *Supplementary Material*. The last term in (2) is calculated as a residual of the other terms that can be derived from observations with its uncertainty being overwhelmingly dominated by that of $\Delta H_2O_{[e]}$. Hence the other uncertainties (including possible non-conservation of total water) are not critical.

References

1. Fu, Q. *et al*. Contribution of stratospheric cooling to satellite-inferred tropospheric temperature trends. *Nature* **429**, doi:10.1038/nature02524 (2004).
2. Cowtan, K. & Way, R. G. Coverage bias in the HadCRUT4 temperature series and its impact on recent temperature trends. *Q. J. R. Meteorol. Soc.* doi: 10.1002/qj.2297 (2014).
3. Forster, P. M. & Shine, K. P. Stratospheric water vapour changes as a possible contributor to observed stratospheric cooling. *Geophys. Res. Lett.* **26**, 3309–3312 (1999).
4. Manabe, S. & Strickler, R. F. Thermal equilibrium of the atmosphere with a convective adjustment. *J. Atmos. Sci.* **21**, 361–385 (1964).
5. Forster, P. M. & Shine, K. P. Assessing the climate impact of trends in stratospheric water vapor. *Geophys. Res. Lett.* **29**, 1086, doi:10.1029/2001GL013909 (2002).
6. Maycock A. C. *et al*. The circulation response to idealized changes in stratospheric water vapor. *J. Clim.,* doi:10.1175/JCLI-D-12-00155.1 (2012).
7. Riese, M. *et al*. Impact of uncertainties in atmospheric mixing on simulated UTLS composition and related radiative effects. *J. Geophys. Res.* **117**, D16305, doi: 10.1029/2012JD017751 (2012).
8. Oltmans, S. J. *et al*. The increase in stratospheric water vapor from balloonborne, frostpoint hygrometer measurements at Washington, D.C., and Boulder, Colorado. *Geophys. Res. Lett.* **27**, doi:10.1029/2000GL012133 (2000).
9. Scherer, M. *et al*. Trends and variability of midlatitude stratospheric water vapour deduced from the re-evaluated Boulder balloon series and HALOE. *Atmos. Chem. Phys.* **8**, 1391–1402, doi:10.5194/acp-8-1391-2008 (2008).
10. Hurst, D. *et al*. Stratospheric water vapor trends over Boulder, Colorado: Analysis of the 30 year Boulder record. *J. Geophys. Res.* **116**, D02306, doi:10.1029/2010JD015065 (2011).
11. Rohs, S. *et al*. Long-term changes of methane and hydrogen in the stratosphere in the period 1978–2003 and their impact on the abundance of stratospheric water vapor. *J. Geophys. Res*. **111**, D14315, doi:10.1029/2005JD006877 (2006).
12. Gettelman, A. *et al*. Multimodel assessment of the upper troposphere and lower stratosphere: Tropics and global trends. *J. Geophys. Res*. **115**, D00M08, doi:10.1029/2009JD013638 (2010).
13. Seidel, D. J. *et al*. Climatological characteristics of the tropical tropopause as revealed by radiosondes. *J. Geophys. Res*. **106**, 7857–7878, doi:10.1029/2000JD900837 (2001).
14. Wang, J. S., Seidel, D. J. & Free, M. How well do we know recent climate trends at the tropical tropopause? *J. Geophys. Res*. **117**, D09118, doi:10.1029/2012JD017444 (2012).

15. Randel, W.J. et al. Interannual changes of stratospheric water vapor and correlations with tropical tropopause temperatures. *J. Atmos. Sci.* **61**, 2133-2148, doi:10.1175/1520-0469(2004)061<2133:ICOSWV>2.0.CO;2 (2004).
16. Fueglistaler, S. et al. The relation between atmospheric humidity and temperature trends for stratospheric water. *J. Geophys. Res.* **118**, 1052–1074, doi:10.1002/jgrd.50157 (2013).
17. Randel, W. J. & Jensen, E. J. Physical processes in the tropical tropopause layer and their roles in a changing climate. *Nature Geoscience* **6,** 169–176, doi:10.1038/ngeo1733 (2013).
18. Hartmann, D.L. et al. Observations: Atmosphere and Surface. In: Climate Change 2013: The Physical Science Basis. Contribution of Working Group I to the Fifth Assessment Report of the Intergovernmental Panel on Climate Change [Stocker, T.F., D. Qin, G.-K. Plattner, M. Tignor, S.K. Allen, J. Boschung, A. Nauels, Y. Xia, V. Bex and P.M. Midgley (eds.)]. Cambridge University Press, Cambridge, United Kingdom and New York, NY, USA (2013).
19. Fueglistaler, S. & Haynes, P. H. Control of interannual and longer-term variability of stratospheric water vapor. *J. Geophys. Res.* **110**, D24108, doi:10.1029/2005JD006019 (2005).
20. Fujiwara, M. et al. Seasonal to decadal variations of water vapor in the tropical lower stratosphere observed with balloon-borne cryogenic frost point hygrometers. *J. Geophys. Res.* **115**, D18304, doi:10.1029/2010JD014179 (2010).
21. Dee, D. P. et al. The ERA-Interim reanalysis: configuration and performance of the data assimilation system. *Q. J .R. Meteorol. Soc.* **137**, 553–597, doi: 10.1002/qj.828 (2011).
22. Voemel, H., David, D. E. & Smith, K. Accuracy of tropospheric and stratospheric water vapor measurements by the cryogenic frost point hygrometer: Instrumental details and observations. *J. Geophys. Res.* **112**, D08305, doi:10.1029/2006JD007224 (2007).
23. Hegglin, M. I. et al. SPARC Data Initiative: Comparisons of water vapour climatologies from international satellite limb sounders. *J. Geophys. Res.* **118**, 11824-11846, doi:10.1029/2013JD019614 (2013).
24. Simmons, A. J. et al. Estimating low-frequency variability and trends in atmospheric temperature using ERA-Interim. *Q.J.R. Meteorol. Soc.* **140**, 329-353. doi: 10.1002/qj.2317 (2014).
25. Thomason, L. W. et. al. A revised water vapor product for the Stratospheric Aerosol and Gas Experiment (SAGE) II version 6.2 data set, *J. Geophys. Res.***109**, D06312, doi:10.1029/2003JD004465 (2004).
26. Fueglistaler, S., Stepwise changes in stratospheric water vapor? *J. Geophys. Res.* **117,** D13302, doi:1029/2012JD017582 (2012).
27. Rosenlof, K. H. & Reid, G. C. Trends in the temperature and water vapor content of the tropical lower stratosphere: Sea surface connection. *J. Geophys. Res.* **113**, D06107, doi:10.1029/2007JD009109 (2008).

28. Randel, W. J. Variability and trends in stratospheric temperature and water vapor. *The Stratosphere: Dynamics, Transport and Chemistry*, S. Polvani, and Waugh, Eds., American Geophysical Union, 123-135 (2010).
29. Kelly, K. K. et al. Dehydration in the lower Antarctic stratosphere during late winter and early spring, 1987. *J. Geophys. Res.* **94**, 317–11,357 (1989).
30. Solomon, S. et al. Contributions of stratospheric water vapor changes to decadal variation in the rate of global warming. *Science* **327**, 1219–1222, doi:10.1226/science.1182488 (2010).
31. Jones, A. et al. Evolution of stratospheric ozone and water vapour time series studied with satellite measurements. *Atmos. Chem. Phys.* **9**, 6055-6075, doi:10.5194/acp-9-6055-2009, 2009 (2012).
32. Garfinkel, C. I., D. W. Waugh, L. D. Oman, L. Wang, & M. M. Hurwitz. Temperature trends in the tropical upper troposphere and lower stratosphere: Connections with sea surface temperatures and implications for water vapor and ozone. *J. Geophys. Res.* **118**, 9658–9672, doi:10.1002/jgrd.50772 (2013).
33. Le Texier, H., Solomon, S., & Garcia, R. R. The role of molecular hydrogen and methane oxidation in the water vapor budget of the stratosphere. *Q. J. R. Meteorol. Soc.* **114**, 281-295 (1988).
34. Dessler, A.E. et al. An examination of the total hydrogen budget of the lower stratosphere. *Geophys. Res. Lett*. **21**, 2563-2566 (1994).
35. Ray, E. A. et al. Evidence for changes in stratospheric transport and mixing over the past three decades based on multiple data sets and tropical leaky pipe analysis. *J. Geophys. Res.* **115**, D21304, doi:10.1029/2010JD014206 (2010).
36. Engel, A. et al. Age of stratospheric air unchanged within uncertainties over the past 30 years. *Nat. Geosci.* **2**, 28–31, doi:10.1038/Ngeo388 (2009).
37. Bönisch, H., Engel, A., Birner, T., Hoor, P., Tarasick, D. W., & Ray, E. A. On the structural changes in the Brewer-Dobson circulation after 2000. *Atmos. Chem. Phys.* **11**, 3937-3948, doi:10.5194/acp-11-3937-2011 (2011).
38. Butchart, N. et al. Chemistry–climate model simulations of twenty-first century stratospheric climate and circulation changes. *J. Climate* **23**, 5349–5374, doi:10.1175/2010JCLI3404.1 (2010).
39. McLandress, C. & Shepherd, T. G. Simulated anthropogenic changes in the Brewer-Dobson circulation, including its extension to high latitudes. *J. Clim.* **22**, 1516–1540 (2009).
40. Scinocca, J. F. et al. Technical Note: The CCCma third generation AGCM and its extension into the middle atmosphere. *Atmos. Chem. Phys.* **8**, 7055-7074, doi:10.5194/acp-8-7055-2008 (2008).
41. Jensen, E. J. et al. Ice nucleation and dehydration in the Tropical Tropopause Layer. *P. Natl. Acad. Sci.* **110**, 2041–2046, doi:10.1073/pnas.1217104110 (2013).

42. Hegglin, M. I. et al. Multimodel assessment of the upper troposphere and lower stratosphere: Extratropics. *J. Geophys. Res.* **115**, D00M09, doi:10.1029/2010JD013884 (2010).
43. Toohey, M. et al. Characterizing sampling biases in the trace gas climatologies of the SPARC Data Initiative. *J. Geophys. Res.* **118**, doi:10.1002/jgrd.50874 (2013).
44. Damadeo, R. P. et al. SAGE version 7.0 algorithm: application to SAGE II. *Atmos. Meas. Tech.* **6**, 3539-3561, doi:10.5194/amt-6-3539-2013 (2013).
45. De Mazière, M. et al. Validation of ACE-FTS v2.2 methane profiles from the upper troposphere to the lower mesosphere. *Atmos. Chem. Phys.* **8**, 2421-2435, doi:10.5194/acp-8-2421 (2008).
46. Hurst, D.F. et al. Validation of Aura Microwave Limb Sounder stratospheric water vapor measurements by the NOAA frost point hygrometer. *J. Geophys. Res*. **119**, doi:10.1002/2013JD020757 (2014).
47. Santer, B. D. et al. Statistical significance of trends and trend differences in layer-average atmospheric temperature time series. *J. Geophys. Res.* **105**, 7337–7356 (2000).